Inorg. Chem. **2006**, *45*, 9696–9702

$CsR(R_6CoI_{12})_2$ (R = Gd, Er) and $(CeI)_{0.26}(Ce_6MnI_9)_2$: Two New Structure Types Featuring R_6Z Clusters

Lucas E. Sweet and Timothy Hughbanks*

Department of Chemistry, Texas A&M University, P.O. Box 30012, College Station, Texas 77842-3012

Received March 14, 2006

Compounds adopting two new structure types containing discrete lanthanide clusters have been found, $CsR(R_6CoI_{12})_2$ (R = Gd or Er) and $(CeI)_{0.26}(Ce_6MnI_9)_2$. $CsEr(Er_6CoI_{12})_2$ and $CsGd(Gd_6CoI_{12})_2$ were synthesized in reactions of CsI, RI_3, CoI_2, and R metals (3:19:6:23) heated to 750 °C for 500 h followed by slow cooling (0.1 °C/min). The X-ray crystal structure of $CsEr(Er_6CoI_{12})_2$ was solved in the $Pa\bar{3}$ space group with $a = 18.063(2)$ Å at 250 K ($Z = 4$, R_1 [$I > 2\sigma(I)$] = 0.0459). $(CeI)_{0.26}(Ce_6MnI_9)$ was synthesized by combining KI, CeI_3, MnI_2, and Ce metal and heating to 850 °C for 500 h. The single-crystal X-ray structure for $(CeI)_{0.26}(Ce_6MnI_9)_2$ was solved in the trigonal, $P\bar{3}$ (147) space group with lattice parameters of $a = 11.695(1)$ Å and $c = 10.8591(2)$ Å ($Z = 2$, R_1 [$I > 2\sigma(I)$] = 0.0895). Elemental analyses (X-ray photoelectron spectroscopy (XPS) and atomic absorption spectroscopy (AAS)) were performed and show the absence of potassium in the structure. A disorder model was refined for the atoms in the large cavity. The magnetic susceptibility data for $CsGd(Gd_6CoI_{12})_2$ is consistent with strong intracluster ferromagnetic coupling, but intercluster antiferromagnetic coupling suppresses the susceptibility below 70 K.

Introduction

We have embarked on a search for new compounds containing discrete lanthanide clusters, spurred by our predictions concerning the effect that d−f exchange interactions have on the magnetic properties of these clusters.[1] However, synthetic challenges must be overcome before we can formulate trends in the properties of these compounds; we currently lack sufficient synthetic control to exploit these compounds' promising magnetic properties. The approach taken here has been to modify reaction conditions for making known compounds in order to expand our inventory of cluster compounds with known (or new) structures. We place our emphasis on finding conditions and compositions that may yield discrete clusters so that structural isolation will enable us to study the magnetic properties of isolated polynuclear lanthanide clusters. There were 10 known structure types for lanthanide iodide compounds that contained uncondensed octahedral clusters, $R(R_6ZI_{12})$,[2] $A_xR_{1-x}(R_6ZI_{12})$,[3−5] $K_2La_6OsI_{12}$,[6] α,β-$K_4La_6OsI_{14}$,[7,8] R_6ZI_{10},[9] $R_{12}M_2I_{17}$,[10,11] $Cs_4R_6ZI_{13}$,[12,13] AR_6ZI_{10},[14] and $CsEr_6CI_{12}$.[15,16] When attempting to make analogues of $Cs_4R_6ZI_{13}$ and α-$K_4La_6OsI_{14}$, we discovered two new structure types: $CsR(R_6CoI_{12})_2$ (R = Er, Gd) and $(CeI)_{0.26}(Ce_6MnI_9)$.

Experimental Section

Synthesis. All manipulations of reactants and products were performed in a N_2-filled glovebox. The title compounds were synthesized in welded Nb tubes sealed in evacuated fused silica jackets. The rare earth triiodides were prepared by oxidation of the rare earth elements with HgI_2, as described in the literature,

* To whom correspondence should be addressed. E-mail: trh@mail.chem.tamu.edu.

(1) Roy, L.; Hughbanks, T. *J. Solid State Chem.* **2003**, *176*, 294−305.
(2) Hughbanks, T.; Corbett, J. D. *Inorg. Chem.* **1988**, *27*, 2022−2026.
(3) Uma, S.; Corbett, J. D. *J. Solid State Chem.* **2001**, *161*, 161−165.
(4) Jensen, E. A.; Corbett, J. D. *Inorg. Chem.* **2002**, *41*, 6199−6205.
(5) Jensen, E. A.; Corbett, J. D. *J. Solid State Chem.* **2003**, *172*, 132−137.
(6) Uma, S.; Corbett, J. D. *Inorg. Chem.* **1998**, *37*, 1944−1948.
(7) Uma, S.; Martin, J. D.; Corbett, J. D. *Inorg. Chem.* **1999**, *38*, 3825−3830.
(8) Uma, S.; Corbett, J. D. *Inorg. Chem.* **1999**, *38*, 3831−3835.
(9) Hughbanks, T.; Corbett, J. D. *Inorg. Chem.* **1989**, *28*, 631−635.
(10) Lulei, M.; Martin, J. D.; Corbett, J. D. *J. Solid State Chem.* **1996**, *125*, 249−254.
(11) Park, Y.; Corbett, J. D. *Inorg. Chem.* **1994**, *33*, 1705−1708.
(12) Lulei, M.; Corbett, J. D. *Inorg. Chem.* **1996**, *35*, 4084−4086.
(13) Artelt, H. M.; Schleid, T.; Meyer, G. *Z. Anorg. Allg. Chem.* **1994**, *620*, 1521−1526.
(14) Lulei, M.; Corbett, J. D. *Z. Anorg. Allg. Chem.* **1996**, *622*, 1677−1684.
(15) Artelt, H. M.; Schleid, T.; Meyer, G. *Z. Anorg. Allg. Chem.* **1992**, *618*, 18−25.
(16) Artelt, H. M.; Meyer, G. *J. Chem. Soc., Chem. Commun.* **1992**, 1320−1321.

10.1021/ic060439d CCC: $33.50
Published on Web 10/31/2006

and purified in at least three vacuum sublimations.[17,18] Transition metal iodides were prepared from the elements and sublimed under static vacuum. CsI (Aesar 99%) and KI (Fisher Scientific 99.95%) were sublimed under dynamic vacuum and stored in ampules before use. The rare earth metals were obtained from Stanford Materials (Gd = 99.95% REM, Ce = 99.9% REM) in ingot form. Turnings were made from the metal ingots by drilling the ingots (in a glovebox) using tungsten carbide drill bits, then collected and stored in evacuated ampules until their use.

$CsGd(Gd_6CoI_{12})_2$ was first discovered in a reaction where CsI, GdI_3, CoI_2, and Gd turnings were ground with a mortar and pestle in the ratio intended to make a compound with the composition "$Cs_4(Gd_6CoI_{14})$". The reactants were heated to 750 °C from room temperature at a rate of 6 °C/h and then maintained at 750 °C for 600 h. The furnace was then turned off and allowed to cool to room temperature. The product contained black, cube-like crystals, which were determined to be $CsR(R_6CoI_{12})_2$ by single-crystal X-ray diffraction. The use of a 3CsI:19GdI_3:6CoI_2:23Gd reactant ratio (~8% rich in Gd for the intended product) in a reaction heated to 750 °C for 21 days, followed by slow cooling (4.5 °C/h) to 300 °C, yielded a product containing ~95% $CsGd(Gd_6CoI_{12})_2$ and ~5% GdOI. An exactly analogous reaction designed to synthesize the Er analogue resulted in the formation of $CsEr(Er_6CoI_{12})_2$ (~50%) and unknown phases.

$(CeI)_{0.26}(Ce_6MnI_9)_2$ was found in reactions loaded with KI, CeI_3, MnI_2, and Ce metals in ratios intended to make "$K_x(Ce_6MnI_{12+y})$". In most of these reactions, $(CeI)_{0.26}(Ce_6MnI_9)_2$ was found in the product as black, plate-like, or multifaceted crystals. Reactions that yielded $(CeI)_{0.26}(Ce_6MnI_9)_2$ were conducted at 850 °C for 500 h by first raising the temperature from ambient at a rate of 7 °C/h. The reaction tube was then cooled at a rate of 6 °C/h to 300 °C, at which time the furnace was turned off. X-ray powder patterns of the reactions loaded at the composition "$KCe_{12}Mn_2I_{18}$" contained a small percentage (5−10%) of $(CeI)_{0.26}(Ce_6MnI_9)_2$, along with CeOI and other unidentified phase or phases.

X-ray Structure Determinations. For $CsGd(Gd_6CoI_{12})_2$ and $(CeI)_{0.26}(Ce_6MnI_9)_2$, single-crystal X-ray data was collected using a Bruker SMART 1000 CCD X-ray diffractometer equipped with graphite monochromated Mo K_α radiation (λ = 0.710 73 Å). A Bruker Apex CCD X-ray diffractometer was used to collect data for $CsEr(Er_6CoI_{12})_2$. Crystals of $CsGd(Gd_6CoI_{12})_2$ and $(CeI)_{0.26}(Ce_6MnI_9)_2$ were mounted on nylon loops using Apeizon N grease and then placed in a N_2 stream at 110 K for data collection; for $CsEr(Er_6CoI_{12})_2$, Paratone oil was used to mount the crystal, and the N_2 stream was set at 250 K. Frame data was indexed using SMART software,[19] and the peak intensities were integrated using SAINT software.[20] Absorption corrections were made using SADABS software.[21] The SHELXTL version 6.10 software package[22] was used as an interface to the SHELX-97 suite of programs,[23] which was used to implement structure solutions by direct methods and full-matrix least-squares structural refinements on F^2.

A black crystal of $CsGd(Gd_6CoI_{12})_2$ with the dimensions 0.06 × 0.02 × 0.02 mm^3 was mounted on the diffractometer, and 29 945 reflections were collected. The data was indexed with a cubic cell and assigned to the $Pa\bar{3}$ space group. However, the data exhibited 31 systematic absence violations, and the refinement showed a residual Fourier peak of 4.19 e Å^3, which formed an octahedron surrounding the Cs atoms at a distance of 2.874 Å. Attempts to identify and resolve a twin relationship by use of Gemini,[24] CellNow,[25] Platon,[26] and twin suggestions from XPREP[22] were unsuccessful. Disorder models could not be refined either. The same problems occurred in the course of the structure solution of one crystal of $CsEr(Er_6CoI_{12})_2$. The R_1 values were 0.0684 and 0.0617 ($I > 2\sigma(I)$) for $CsEr(Er_6CoI_{12})_2$ and $CsGd(Gd_6CoI_{12})_2$, respectively. The structure solution for a second crystal of $CsEr(Er_6CoI_{12})_2$ at 250 K was solved in the $Pa\bar{3}$ space group; the data exhibited six weak ($6\sigma(I) \gtrsim I$) systematic absence violations. The final residual was 0.0459 ($I > 2\sigma(I)$) (Table 1).

Table 1. Crystallographic Data for $CsEr(Er_6CoI_{12})_2$ and $(CeI)_{0.26}(Ce_6MnI_9)_2$

	$CsEr_{13}Co_2I_{24}$	$Ce_{6.13}MnI_{9.13}$
fw (g/mol)	5470.75	2072.34
temp (K)	250(2)	110(2)
crys sys, space group, Z	cubic, $Pa\bar{3}$ (no. 205), 4	trigonal, $P\bar{3}$ (no. 147), 2
lattice param (Å)	18.063(2)	11.695(1), 10.859(2)
V (Å^3)	5893.8(12)	1286.3(3)
density (calcd) (g/cm^3)	6.165	5.351
abs coefficient (mm^{-1})	32.008	21.993
extinction coefficient	3.4(4) × 10^{-5}	
final R indices [$I > 2\sigma(I)$]	$R_1{}^a$ = 0.0459, $wR_2{}^b$ = 0.0932	$R_1{}^a$ = 0.0895, $wR_2{}^c$ = 0.1868
R indices (all data)	$R_1{}^a$ = 0.0701, $wR_2{}^b$ = 0.1019	$R_1{}^a$ = 0.1239, $wR_2{}^c$ = 0.2032

[a] $R_1 = \sum||F_o| - |F_c||/\sum|F_o|$. [b,c] $wR_2 = \{\sum[w(F_o^2 - F_c^2)^2]/\sum[w(F_o^2)^2]\}^{1/2}$, where [b] $w = 1/[\sigma^2(F_o^2) + (0.0386P)^2 + (33.2546P)]$ and [c] $w = 1/[\sigma^2(F_o^2) + (0.\ 0797P)^2 + (61.5001P)]$, $P = (F_o^2 + 2F_c^2)/3$.

A black multifaceted crystal of $(CeI)_{0.26}(Ce_6MnI_9)_2$, with the dimensions 0.11 × 0.12 × 0.12 mm^3, was mounted on the diffractometer, and 20 216 reflections were collected and indexed in the $P\bar{3}$ space group. During the data collection, the crystal mounting pin obstructed the X-ray beam path, causing a series of consecutive frames to be void of diffraction peaks from the crystal. The frames affected by the obstruction were not included in the data used to solve the structure. The basic structure emerged from direct methods and was refined without difficulty, but two electron density peaks remained in an otherwise vacant cuboctahedral cavity created by the clusters. Because there were no unindexed reflections, no twinning beyond that by merohedry was deemed possible. After attempting every merohedral twin model suggested by XPREP[22] without making any headway, we considered disorder models—see discussion section. The most reasonable model was to restrain the noncluster Ce and I to have the same occupancy factor. This resulted in 26% of the cavities containing additional cerium and iodide ions, leaving the remaining cavities vacant.

Elemental Analysis. To establish whether potassium was present in $(CeI)_{0.26}(Ce_6MnI_9)_2$, X-ray photoelectron spectra (XPS) were recorded on a Kratos Axis Ultra Imaging X-ray photoelectron spectrometer equipped with an Al anode and a multichannel detector. Charge referencing was performed against adventitious

(17) Corbett, J. D. *Inorg. Synth.* **1983**, *22*, 31−36.
(18) Corbett, J. D. *Inorg. Synth.* **1983**, *22*, 15−22.
(19) SMART-V5.625: Program for Data Collection on Area Detectors. Bruker AXS Inc.: Madison, WI, 2001.
(20) SAINT-V6.63: Program for Reduction of Area Detector Data. Bruker AXS Inc.: Madison, WI, 2001.
(21) Sheldrick, G. M. SADABS-V2.03: Program for Absorption Correction of Area Detector Frames. Bruker AXS Inc.: Madison, WI, 2001.
(22) SHELXTL-V6.12 (PC-version): Program for Structure Solution, Refinement and Presentation. Bruker AXS Inc.: Madison, WI, 2000.
(23) Sheldrick, G. M. SHELXL-97: Program for Crystal Structure Refinement. Institüt für Anorganische Chemie der Universität: Gottingen, Germany, 1997.
(24) GEMINI−V1.02: Program for Twin Deconvolution. Bruker AXS Inc.: Madison, WI, 2000.
(25) Sheldrick, G. M. CELLNOW: Program for Unit Cell Determination. Institüt für Anorganische Chemie der Universität: Gottingen, Germany, 2003.
(26) Spek, A. L. *J. Appl. Crystallogr.* **2003**, *36*, 7−13.

carbon (C 1s, 284.5 eV). Samples were prepared by picking crystals (of like morphology) from reaction product mixtures from which crystals for X-ray structure determination were taken. XPS measurements were performed on two different samples. Potassium was not detected in either of the samples. The K/Mn atomic ratio for a benchmark $KMnCl_3$ sample was determined to be 56:44.

Atomic absorption (AA) spectroscopy was also used to determine the possible presence of potassium; crystals were selected in the same manner as those used for XPS measurements. The 3.3 mg sample was dissolved in 0.048 M HCl (5.0 mL) and analyzed on a Varian 250 AA system. The same HCl solution was used as the blank. The potassium content of the sample was not determined to be significantly different from the blank.

Magnetic Measurements. Magnetic measurements were performed with a Quantum Design SQUID magnetometer MPMSXL on a polycrystalline sample of $CsGd(Gd_6CoI_{12})_2$. Temperature-dependent magnetization data were collected at 5−10 K intervals from 10−300 K in applied fields of 0.1, 0.5, 1.0, 2.0, and 3.0 T. All data were corrected for the sample holder and the intrinsic diamagnetic contributions.[27]

Results and Discussion

Synthesis. As indicated in the Experimental Section, $CsGd(Gd_6CoI_{12})_2$ is a stable phase that can be prepared in a yield that is less than quantitative only because it is difficult to entirely avoid oxygen-containing impurities. Thus, a modest excess of gadolinium is necessary to obtain the best practical results. For the erbium analogue, $CsEr(Er_6CoI_{12})_2$, our yields never exceeded the 50% reported here. Variations in stoichiometry and reaction temperatures were to no avail. The competing (and well-known) structure type, $Er(Er_6CoI_{12})$, is often observed as the major side product of such attempts. We are very much interested in varying the magnetic properties of these compounds and so were motivated to incorporate Fe, Mn, and Ni as interstitial atoms in compounds of this type, but such attempts resulted in the formation of $R(R_6ZI_{12})$, unreacted CsI, and other unidentified phases.

$(CeI)_{0.26}(Ce_6MnI_9)_2$ was found in several reactions loaded with KI, CeI_3, MnI_2, and Ce metal in ratios intended to target Ce analogues of α- or β-$K_4La_6OsI_{14}$,[7,8] and new compounds with $K_x(Ce_6MnI_{12+y})$ compositions. Despite the absence of potassium in this compound, we have so far only definitively observed this product in reactions including KI. Reactions loaded with CeI_3, MnI_2, and Ce metal in ratios at and near the "Ce_6MnI_9" composition yielded similar black, plate-like crystals, but these diffracted poorly. Powder diffraction data did not indicate the presence of $(CeI)_{0.26}(Ce_6MnI_9)_2$ when KI was not included in the reactant mixture. Because these reactions were conducted at 850 °C, above the melting point of KI, we speculate that the KI melt may allow nucleation of this phase. The reactions that were loaded with an excess of KI still yielded $(CeI)_{0.26}(Ce_6MnI_9)_2$ and contained white powder in the final product, but KI was not observed in the X-ray powder patterns of the products.

Structure. The $CsR(R_6CoI_{12})_2$ structure type may be viewed as an intergrowth of the $R(R_6CoI_{12})$ and $Cs(Er_6CI_{12})$ structure types; we preface our discussion of the structure with brief remarks concerning these two structures in order to clarify this viewpoint. If we adopt a view wherein the R_6ZI_{12} cluster is aligned with a 3-fold vertical axis, then six of the cluster's bridging iodides may be described as "waist" ligands (girding the center of the cluster at the same "height" as the interstitial Z atom; Z = C, Co). The other six iodide ligands bridge R−R bonds that make up the top and bottom triangular faces of the R_6 trigonal antiprism. In the $R(R_6CoI_{12})$ structure, cluster cross-linking occurs exclusively through the waist iodides, and an $R\bar{3}$ structure is thereby generated. The "top" and the "bottom" iodides on vertically adjacent clusters form opposite triangular faces of a trigonal antiprism in which R^{III} ions are situated (top left, Figure 1). In the $Cs[Er_6CI_{12}]$ structure, cluster cross-linking occurs exclusively via the top and bottom iodides, and all the iodides form cuboctahedral sites for 12-coordinate Cs ions (bottom left, Figure 1). A cubic ($Pa\bar{3}$) intergrowth of these two $R\bar{3}$ structures is generated by aligning the 3-fold axes of the two structures and "fusing" clusters (Figure 1). The full cubic symmetry structure emerges as cluster fusions are performed along nonintersecting 3-fold axes that run through each of the Cs^I and R^{III} ions in the structure. (Only the Cs polyhedron for the ion at (1/2, 1/2, 1/2) is shown; equivalent Cs positions at (1/2, 0, 0), (0, 1/2, 0), and (0, 0, 1/2) are not shown.)

When the $CsGd(Gd_6CoI_{12})_2$ structure was initially determined, refinement in the $Pa\bar{3}$ space group was accompanied by difficulties symptomatic of twinning by merohedry: all reflections could be indexed, but there were numerous systematic absence violations of significant intensity, and spurious peaks in the electron density persisted in the refined structure (e.g., a trigonal antiprism of electron density peaks, each ∼4 e $Å^{-3}$, with dimensions similar to a Gd_6 cluster surrounding the Cs site). Various disorder models and twin laws were attempted, but no simple twinning sufficed; more than one twin domain was probably present in this cubic case. The first several crystals obtained for $CsEr(Er_6CoI_{12})_2$ exhibited the same characteristics. Fortunately, a crystal of $CsEr(Er_6CoI_{12})_2$ where these problems were minimal was found (six systematic absence violations were observed, but the peak intensities were quite weak, $(6\sigma(I) \gtrsim I)$.

In the structure of $(CeI)_{0.26}(Ce_6MnI_9)_2$, each cluster is centered on a 3-fold axis and is linked to six neighboring clusters through bridging iodides. Three clusters are linked through I^{i-i}, I^{i-a}, and I^{a-i} bridges; the other three clusters are linked by I^{i-a} and I^{a-i} bridges. Thus, the structure can be viewed as layers of tightly cross-linked clusters (three iodine bridges) and the layers are joined by loose cross-linking (two iodine bridges), as shown in Figure 2. The resulting connectivity can be described as $(CeI)_{0.26}(Ce_6Mn)I^{i-i}{}_{6/2}I^{i-a}{}_{6/2}I^{a-i}{}_{6/2}$. The Mn−Mn distances within the layers are 7.677 Å, whereas the Mn−Mn distances between the layers are 9.875 Å. The cavities are partially occupied by Ce−I units. The Ce atoms of the Ce−I units are disordered over six equivalent positions. When the structure is viewed down the *c* axis, as in Figure 3, the cavities stack upon each other to form channels.

The structure was solved twice with data from two different crystals obtained from two different reactions. The

(27) Kahn, O. *Molecular Magnetism*; VCH: New York, 1993.

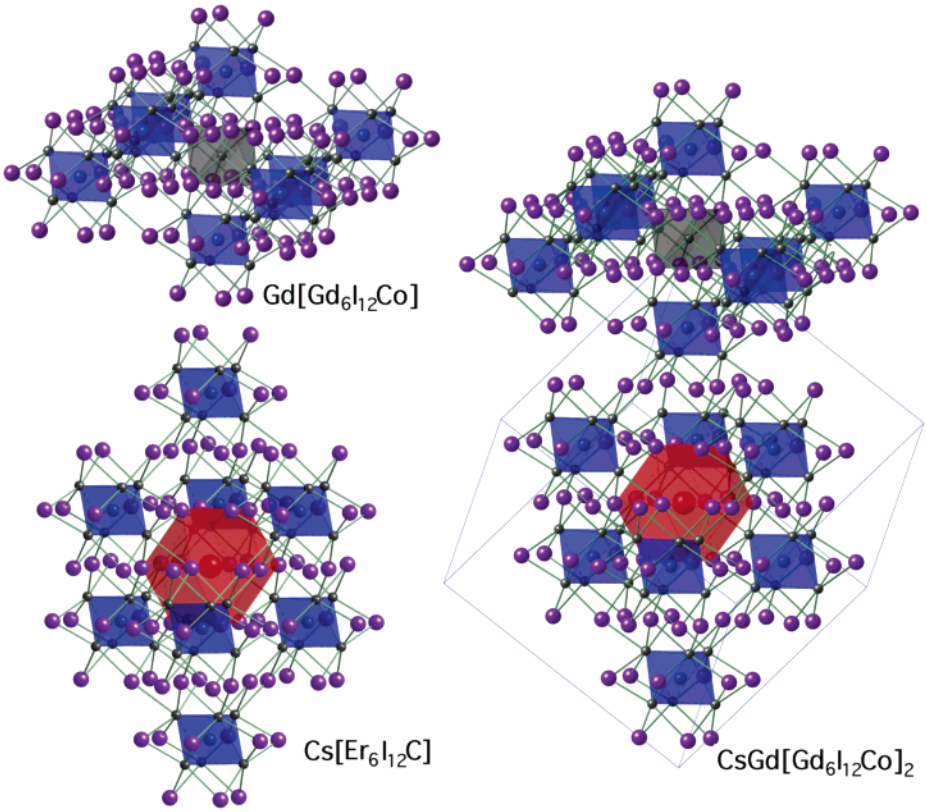

Figure 1. Structural relationship between $Gd[(Gd_6Co)I_{12}]$, $Cs[(Er_6C)I_{12}]$, and $CsGd[(Gd_6Co)I_{12}]_2$. The blue octahedra represent the Ln_6Z (Z = Co or C) units. The red cuboctahedron is a CsI_{12} coordination polyhedron, and the $Gd^{III}I_6$ octahedron is gray.

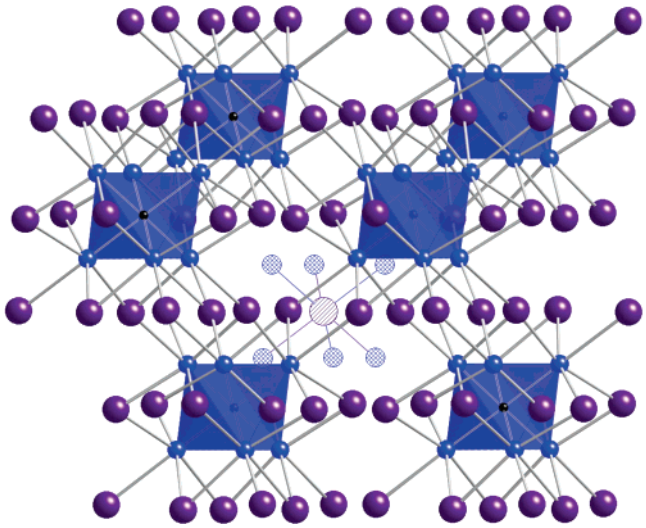

Figure 2. View through the [011] plane of $(CeI)_{0.26}(Ce_6MnI_9)_2$; Ce_6Mn cores are represented as blue trigonal antiprisms, and the iodine atoms are purple. The sites of disorder in the cavity are shown as hatched and striped circles for Ce(3) and I(4), respectively. Only one set of sites of disorder is shown for clarity.

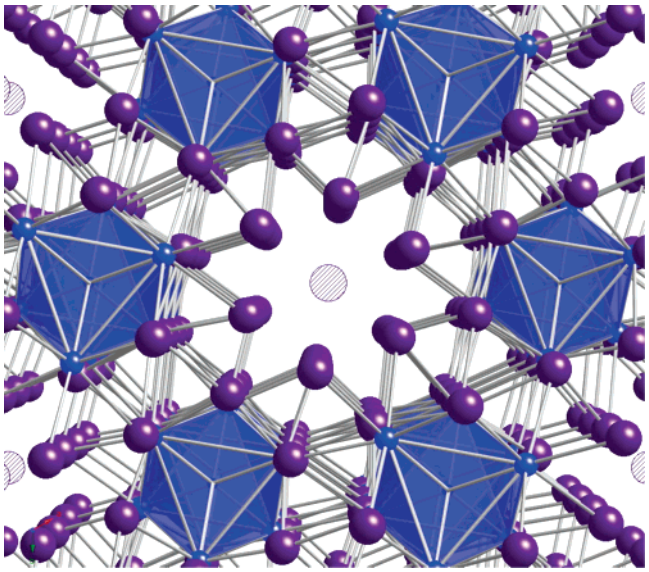

Figure 3. View down the *c* axis of $(CeI)_{0.26}(Ce_6MnI_9)_2$; cluster and atom color scheme are as in Figure 2. The iodine atoms that form the cavity obscure the noncluster Ce atoms.

first solution came from the smaller data set (6136 reflections, $2\theta < 56°$). This solution yielded better residuals than those published here: $R_1 = 0.050$ ($F_o > 4\sigma(F_o)$), and the CeI occupancy of the cavity sites was refined to 24%. Concerned that the electron density peaks in the cavity might be artifacts attributable to truncation error, we collected a second, larger set of data (20 216 reflections, $2\theta < 68°$). However, virtually the same solution was obtained, albeit with larger residual peaks (~8 e $Å^{-3}$, located 0.5 Å distant from Ce1) after the final solution. Despite the somewhat poorer residuals for this solution ($R_1 = 0.089$), we elected to report the results obtained for this larger data set.

We initially refined the structure with potassium occupying the two sites in the cavity, in light of a report that potassium occupies a large cavity in a similar compound, KPr_6OsI_{10}.[14] However, because XPS and AA results indicated that there is no potassium in the structure, a new disorder model containing cerium and iodine was used.

After refining the clusters, the center position of the cavity exhibited a significant residual electron density peak. Because cerium is far too small to occupy this position, iodine was assigned to it. The distances from the center of the cavity and the edge bridging iodine atoms of the clusters (6×4.31 and 6×4.42 Å) are longer than twice the *Shannon* crystal radius for 6-coordinate I^- (4.06 Å).[28] Because an unbound iodide ion is chemically unreasonable, a cerium atom was refined in the general position(s) that form a trigonal antiprism around the central I atom. The distance from this cerium atom to the nearest iodine atoms ranges 2.94−3.15 Å, which is short compared with the $Ce^{3+}-I^-$ distance (Ce^{4+} is chemically precluded in this reduced compound) calculated from *Shannon crystal radii*[28] (3.34 Å).

The Fourier peaks for the two positions in the cavity indicate the electron density on both positions fell far short of that needed for full occupancy of the sites. The disorder model used in the refinement consisted of restraining the occupancy of the noncluster Ce such that its total population in the crystal equaled that of the iodine atoms in the center of the cavity. As a rationalization of this choice, we note that this allows no cavity iodides to remain unbound and allows no 5-coordinate cerium. This refinement model yielded a 26% occupancy of the cavities by CeI units.[29]

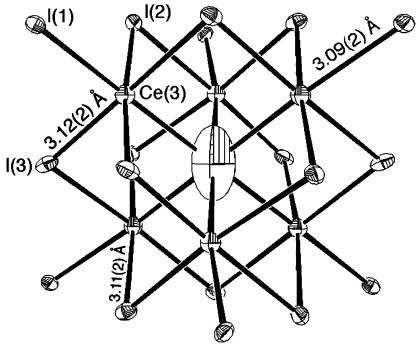

Figure 4. Coordination environment of I(4) (center) and Ce(3) in $(CeI)_{0.26}(Ce_6MnI_9)_2$. Ce(3) was refined isotropically. Ellipsoids are drawn at 60%.

The anisotropic displacement parameters for the Ce atoms in the cavity could not be refined in a physically reasonable way and were therefore left isotropic. The iodine atom refined as a large prolate displacement ellipsoid, but this almost certainly reflects its average position, because there is no reason to believe that the center of the cavity is at the optimal bonding distance with respect to the surrounding Ce positions (Tables 2−5).

Magnetism. Although powder diffraction data indicate that the synthesis of $CsGd(Gd_6CoI_{12})_2$ was nearly quantitative, magnetic measurements revealed the presence of ferromagnetic impurities. By measuring the magnetization as a function of temperature for a series of applied fields, one can determine the extent of the ferromagnetic impurity. By use of stronger applied fields, the contribution of the fractional ferromagnetic impurity to the total susceptibility becomes negligible, as illustrated in Figure 5.

The electronic structure of $[R_6Z]$ clusters (for rare earth and zirconium clusters with main group or transition metal interstitials) have been discussed thoroughly in the past,[2,14,30−35]

Table 2. Atomic Coordinates and Equivalent Isotropic Displacement Parameters ($Å^2 \times 10^3$) for $CsEr(Er_6CoI_{12})_2$

atom	Wyckoff symbol	*x*	*y*	*z*	U_{eq}[a]
Er(1)	24*d*	0.1731(1)	0.3300(1)	0.5241(1)	8(1)
Er(2)	24*d*	0.3141(1)	0.3298(1)	0.6677(1)	7(1)
Er(3)	4*a*	0	0.5000	0.5000	9(1)
I(1)	24*d*	0.1686(1)	0.3356(1)	0.3425(1)	15(1)
I(2)	24*d*	0.4954(1)	0.3332(1)	0.6623(1)	16(1)
I(3)	24*d*	0.3386(1)	0.3356(1)	0.5012(1)	17(1)
I(4)	24*d*	−0.0008(1)	0.3338(1)	0.4973(1)	12(1)
Cs(1)	4*b*	0.5000	0.5000	0.5000	40(1)
Co(1)	8*c*	0.1693(1)	0.3307(1)	0.6693(1)	7(1)

[a] $U_{eq} = (8\pi^2/3)\sum_i\sum_j U_{ij} a_i a_j \vec{a}_i \vec{a}_j$.

Table 3. Selected Interatomic Distances (Å) and Angles (deg) for $CsEr(Er_6CoI_{12})_2$

	distance
Er(1)−Co(1)	2.624(2)
Er(2)−Co(1)	2.615(2)
Er(1)−Er(1)	3.769(1)
Er(2)−Er(2)	3.708(1)
Er(1)−Er(2)	3.707(1)
	3.635(1)
Er(1)−I(1)$^{a-i}$	3.283(1)
Er(1)−I(2)$^{i-a}$	3.075(1)
Er(1)−I(3)^{i}	3.020(1)
Er(1)−I(4)^{i}	3.180(1)
	3.156(1)
Er(2)−I(1)$^{i-a}$	3.075(1)
	3.136(1)
Er(2)−I(2)$^{a-i}$	3.278(1)
Er(2)−I(2)$^{i-a}$	3.185(1)
Er(2)−I(3)^{i}	3.043(1)
Er(3)−I(4)	3.004(1)
Cs(1)−I(2)	4.205(1)
Cs(1)−I(3)	4.161(1)
	angle
I(2)−Er(1)−I(4)	161.57(4)
I(3)−Er(1)−I(4)	163.07(4)
I(1)−Er(2)−I(2)	165.17(4)
I(3)−Er(2)−I(1)	161.84(4)

Table 4. Atomic Coordinates and Equivalent Isotropic Displacement Parameters ($Å^2 \times 10^3$) for $(CeI)_{0.26}(Ce_6MnI_9)$

atom	Wyckoff symbol	*x*	*y*	*z*	U_{eq}[a]	SOF
Ce(1)	6*g*	0.5468(1)	0.70796(9)	0.47641(9)	37.0(3)	1
Ce(2)	6*g*	0.50495(8)	0.87544(8)	0.18216(8)	23.8(2)	1
Ce(3)	6*g*	0.233(2)	0.036(2)	0.1629(19)	29(6)	0.043(4)
I(1)	6*g*	0.47818(8)	0.10598(8)	0.31898(8)	22.1(2)	1
I(2)	6*g*	0.77171(9)	0.96436(9)	0.33649(8)	26.4(2)	1
I(3)	6*g*	0.28490(9)	0.8693(1)	−0.00381(8)	27.1(2)	1
I(4)	1*b*	0	0	0	190(20)	0.26(2)
Mn(1)	2*d*	0.3333	0.6667	0.3318(4)	33.2(9)	1

[a] $U_{eq} = (8\pi^2/3)\sum_i\sum_j U_{ij} a_i a_j \vec{a}_i \vec{a}_j$.

(28) Shannon, R. D. *Acta Crystallogr.* **1976**, *A32*, 751−767.
(29) The following restraint was used in SHELX to refine the occupancy of the cavity: occupancy of CeI units in cavity = *x*(1/6 of this site multiplicity of the (Ce) general position) = *x*′(the site multiplicity of the (I) central position); site multiplicity of the general position = 6, site multiplicity of the central position = 1.
(30) Hughbanks, T.; Rosenthal, G.; Corbett, J. D. *J. Am. Chem. Soc.* **1988**, *110*, 1511−1516.
(31) Hwu, S. J.; Corbett, J. D. *J. Solid State Chem.* **1986**, *64*, 331−346.
(32) Ziebarth, R. P.; Corbett, J. D. *J. Am. Chem. Soc.* **1985**, *107*, 4571−4573.

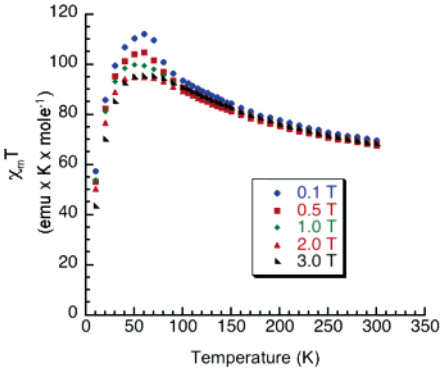

Figure 5. Ferromagnetic impurities are saturated in higher applied fields. There is very little difference between data collected at 2.0 and 3.0 T. The data collected at 3.0 T used a second sample taken from the same reaction product.

Table 5. Selected Atomic Distances (Å) and Angles (deg) for $(CeI)_{0.26}(Ce_6MnI_9)$

	distance
Ce(1)−Ce(1)	3.908(2)
Ce(2)−Ce(2)	3.973(2)
Ce(1)−Ce(2)	3.941(1)
	3.904(2)
Ce(1)−I(1)$^{i-i}$	3.228(1)
Ce(1)−I(2)$^{i-a}$	3.222(1)
Ce(1)−I(3)$^{i-a}$	3.244(1)
	3.194(1)
Ce(1)−I(3)$^{a-i}$	3.372(1)
Ce(2)−I(1)$^{i-i}$	3.224(1)
	3.259(1)
	3.293(1)
Ce(2)−I(2)$^{i-a}$	3.214(1)
Ce(2)−I(2)$^{a-i}$	3.420(2)
Ce(3)−I(1)	3.07(2)
Ce(3)−I(2)	3.14(2)
	3.15(2)
Ce(3)−I(3)	2.94(2)
	3.13(2)
Ce(3)−I(4)	3.10(2)
Ce(1)−Mn	2.780(3)
Ce(2)−Mn	2.780(3)
	angle
I(1)−Ce(2)−I(1)	165.27(5)
I(1)−Ce(2)−I(2)	164.73(5)
I(1)−Ce(1)−I(3)	163.67(4)
I(2)−Ce(1)−I(3)	163.86(4)

but we will briefly review it here in order to assess the magnetism of $CsGd(Gd_6CoI_{12})_2$. In Figure 6, a qualitative molecular orbital diagram for a transition metal-centered gadolinium cluster $[Gd_6ZI_{12}]$ is shown. Because the 4f orbitals of the lanthanide atoms are highly contracted, the diagram includes only orbitals that have significant contribution to the metal−metal bonds (5d/6s orbitals). The 3d (t_{2g}/e_g in O_h symmetry) and 4s (a_{1g}) orbitals of the first row transition metals interact with the cluster orbitals formed by the Gd_6 cage. The filled-shell electronic configuration (t_{1u}^6 highest occupied molecular orbital (HOMO)) is that of $[Gd_6CoI_{12}]^{3-}$, which has 18 electrons in the cluster-bonding

(33) Hughbanks, T.; Rosenthal, G.; Corbett, J. D. *J. Am. Chem. Soc.* **1986**, *108*, 8289−8290.
(34) Smith, J. D.; Corbett, J. D. *J. Am. Chem. Soc.* **1986**, *108*, 1927−1934.
(35) Smith, J. D.; Corbett, J. D. *J. Am. Chem. Soc.* **1985**, *107*, 5704−5711.

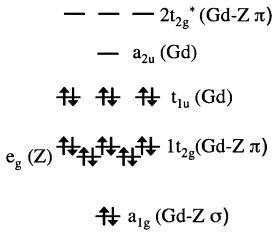

Figure 6. Molecular orbitals of a Gd_6Z cluster with O_h symmetry. With 18 e^-, a closed shell t_{1u} HOMO results.

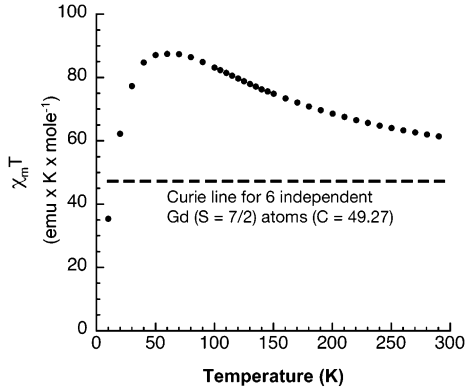

Figure 7. $\chi_m T$ vs T (K) for $CsGd(Gd_6CoI_{12})_2$, corrected to show the molar susceptibility per cluster. The dc applied field was 3.0 T.

orbitals. $CsGd(Gd_6CoI_{12})_2$ contains $[Gd_6CoI_{12}]^{2-}$ clusters and therefore a t_{1u}^5 HOMO configuration.

Although the 4f orbitals do not engage in significant Gd−ligand−Gd superexchange coupling, there is a significant intraatomic exchange interaction between the 4f and the valence 5d and 6s electrons. This intraatomic exchange interaction is the ultimate source of 4f−4f coupling between Gd centers. In clusters with open 5d/6s shells, like $CsGd(Gd_6CoI_{12})_2$, the effects of this spin coupling are enhanced.

The susceptibility plotted is on a per-mole-of-cluster basis. $CsGd(Gd_6CoI_{12})_2$ contains an isolated Gd^{3+} cation, which we assume makes an ideal Curie-like ($S = 7/2$) contribution to the total susceptibility, and we therefore subtract that contribution from the total susceptibility before dividing by 2:

$$\chi_m(Cs_{1/2}Gd_6CoI_{12}^{1.5-}) = 1/2(\chi_m[CsGd(Gd_6CoI_{12})_2) - \chi_m(Gd^{3+})]$$

The susceptibility data is plotted on a per-cluster basis as $\chi_m T$ vs T (Figure 7), where $\chi_m T$ is proportional to μ_{eff}^2 for the cluster via the familiar relationship

$$\chi_m T = (N_{avo}\mu_B^2/3k_B)\mu_{eff}^2$$

Ideal Curie behavior results in a horizontal line were the intercept with the $\chi_m T$ axis is equal to the Curie constant ($C_{Curie} = \chi_m T$). In the absence of magnetic coupling between the $4f^7$ moments (i.e., 6 × 7/2-spins), one would expect $\chi_m T = 47.25$ emu × K × mol^{-1}. The enhanced moment observed is a result of ferromagnetic coupling within the hexanuclear cluster, mediated by the unpaired 5d electron in this open-shell cluster. A discussion of this behavior in the context of

data for other hexanuclear gadolinium clusters is presented elsewhere.[36]

Conclusions

In attempts to find analogues of known $Cs_4R_6ZI_{13}$ and χ-$K_4La_6OsI_{14}$ phases, we have discovered two new structure types of compounds containing reduced Ln−iodide clusters. With only four types of iodine bridges to neighboring octahedral lanthanide clusters (I^{i-i}, I^{a-a}, I^{i-a}, I^{a-i}, or terminal), 12 different structure types have so far been observed. $CsEr(Er_6CoI_{12})_2$ and $CsGd(Gd_6CoI_{12})_2$ adopt a cubic intergrowth of two different $R\bar{3}$ structure types. The channels formed by the cross-linking of the clusters in $(CeI)_{0.26}(Ce_6MnI_9)_2$ may be capable of accommodating a range of cations. Finally, the magnetism of $CsGd(Gd_6CoI_{12})_2$ indicates that there is magnetic coupling between the spins of the electrons in the 4f orbitals of neighboring Gd atoms. Work is currently underway to more fully explain the magnetism of Gd_6ZI_{12}-cluster-containing compounds and to broaden the known range of compounds, with the aim of finding truly discrete Ln−Ln bonded clusters.

Acknowledgment. We thank the Robert A. Welch Foundation for its support through Grant A-1132 and the Texas Advanced Research Program through grant no. 010366-0188-2001. We thank the National Science Foundation for the X-ray diffractometers and crystallographic computing systems in the X-ray Diffraction Laboratory at the Department of Chemistry, Texas A&M University (CHE-9807975), and the SQUID magnetometer (NSF-9974899). We thank Dr. Carmela Magliocchi for her instructions on crystallography and magnetic measurements. We thank an astute reviewer for prompting us to perform XPS and AA measurements and Dr. Sharath Kirumakki for his help in doing so. Use of the TAMU/CIMS Materials Characterization Facility for XPS measurements is acknowledged.

Supporting Information Available: Crystallographic data in CIF format for $CsEr(Er_6CoI_{12})_2$ and $(CeI)_{0.26}(Ce_6MnI_9)_2$. This material is available free of charge via the Internet at http://pubs.acs.org.

IC060439D

(36) Sweet, L. E.; Roy, L. E.; Meng, F.; Hughbanks, T. *J. Am. Chem. Soc.* **2006**, *128*, 10193−10201.